tors p. 372, The Electrochemical Society Softbound Proceedings Series, Vol. 82-3, Pennington, NJ (1982).
35. V. A. Tyagai and G. Ya. Kolbasov, *Surf. Sci.*, **28**, 423 (1971).
36. Kabir-ud-Din, R. C. Owen, and M. A. Fox, *J. Phys. Chem.*, **85**, 1679 (1981).
37. M-S. Lin, N. Hung, and M. S. Wrighton, *J. Electroanal. Chem. Interfacial Electrochem.*, **135**, 121 (1982).
38. K. W. Frese, Jr., *J. Appl. Phys.*, **53**, 1571 (1982).
39. A. M. Van Wezemael, W. H. Laflere, F. Cardon, and W. P. Gomes, *J. Electroanal. Chem. Interfacial Electrochem.*, **87**, 105 (1978).
40. B. Tuck, G. Eftekhari, and D. M. de Cogan, *J. Phys. D: Appl. Phys.*, **15**, 457 (1982).
41. A. K. Ghosh, F. G. Wakim, and R. R. Addiss, Jr., *Phys. Rev.*, **184**, 979 (1969).
42. V. E. Henrich, G. Dresselhaus, and H. J. Zeiger, *Phys. Rev. Lett.*, **36**, 1335 (1976).
43. J. Cunningham and A. L. Penny, *J. Phys. Chem.*, **78**, 870 (1974).
44. K. Kobayashi, Y. Aikawa, and M. Sukigara, *Chem. Lett.*, 679 (1981).
45. W. P. Gomes and F. Cardon, *Ber. Bunsenges. Phys. Chem.*, **74**, 431 (1970).

A Study of the Transition from Oxide Growth to O_2 Evolution at Pt Electrodes in Acid Solutions

V. I. Birss*

Department of Chemistry, University of Ottawa, Ottawa, Ontario, Canada

A. Damjanovic*

Corporate Research and Development, Allied Corporation, Morristown, New Jersey 07960

ABSTRACT

A Pt ring disk electrode was used in acid solutions to study the transition from Pt oxide growth to oxygen evolution and to distinguish the rates of these two processes. When a constant current is applied to the disk electrode, the disk potential, V, initially increases linearly with time, and hence with the charge density, while a negligible current is observed at the ring. In this potential region, essentially all of the applied current is used for the growth of a Pt oxide film. Following the linear V/t region, V continues to increase but now more slowly and nonlinearly with time, while the ring current initially increases sharply and then slowly approaches the value expected for 100% oxygen evolution at the disk electrode. Thus, the Pt oxide film continues to grow in the nonlinear V/t region even when oxygen evolution becomes the major reaction. In the nonlinear V/t region, V again increases nearly linearly with the integrated charge density for oxide film formation or with the oxide film thickness. This V/q relationship in the nonlinear V/t region is different from the V/q relationship in the linear V/t region. However, the mechanism of Pt oxide growth and the properties of the film when the O_2 evolution reaction is the dominant reaction remain the same as in the initial Pt oxide growth region where O_2 evolution is not significant. The distribution of potentials in the oxide film and in the inner and outer Helmholtz layers is discussed.

When a constant anodic current is applied to a prereduced oxide-free Pt electrode starting from the rest potential in O_2-saturated acid or alkaline solutions, $V_R = 0.98$V *vs.* RHE (1), three distinct potential regions can be seen in a V/t transient (2-5). Initially, the potential increases rapidly and nonlinearly with time as the first monolayer of an oxide film is formed (5-7). Following this region, the electrode potential increases fairly linearly with time (Fig. 1) with the current being used for further growth of the oxide film (8). Eventually at higher potentials, oxygen evolution begins and soon becomes the major electrode reaction.

In Fig. 1, potential/time curves are shown for three constant current densities in a $0.2N$ H_2SO_4 solution. In this figure, the time axis has been scaled for each current density to represent charge density, $q = it$. At a particular potential, which depends on the applied current density and the pH, the linear increase of the potential with time, or charge density, ceases. Now, the potential increases at a rate which decreases with time while O_2 evolution continues to increase and soon becomes the predominant electrode reaction (9). Previous work has shown that at long times the potential changes nearly linearly with the logarithm of time of polarization and the oxide film continues to grow at a very slow rate (3, 9, 10).

In this study, a Pt ring disk electrode has been used to separate the reactions of Pt oxide growth and O_2 evolution. A comparative analysis of their individual rates and their dependence on the electrode potential is expected to yield information on the nature of the changes in the kinetics of oxide growth and on the potential distribution across the complex interface, comprised of the oxide film and the inner and outer Helmholtz layers, during the transition from the oxide growth to O_2 evolution. Such an analysis is also expected to aid in the overall understanding of the mechanism of the O_2 evolution reaction at oxide-covered electrodes.

Experimental

A commercially designed Pt disk-Pt ring electrode (Pine Instrument Company, disk radius 0.383 cm, ring inner radius 0.399 cm, and ring outside radius 0.422 cm) was utilized in an all-glass cell similar to that described in (11). The ring-disk electrode was polished to a mirror finish with alumina paste. In some experiments, a thin layer of gold (~1000Å) was electrodeposited over the ring electrode. A saturated calomel electrode in a separate compartment served as the reference electrode, and a Luggin capillary extended upwards toward the center of the disk electrode. A Pt counterelectrode was placed in the same compartment as the ring disk electrode.

Solutions were prepared from reagent grade sulfuric acid and conductivity water. No extensive purification of solutions was carried out, *e.g.*, by preelectrolysis. In all experiments, solutions were first purged of O_2 with high purity Ar. During electrochemical measurements, Ar was passed over the solution.

Prior to each series of experiments, the disk electrode was anodically oxidized and cathodically re-

* Electrochemical Society Active Member.
Key words: metal, kinetics, chemisorption.

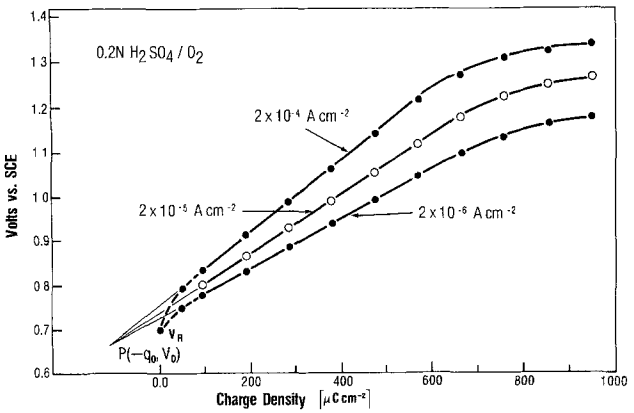

Fig. 1. *V-q* relationships at three constant current densities. Current and charge densities are corrected for surface roughness (wire electrode, RF = 1.6).

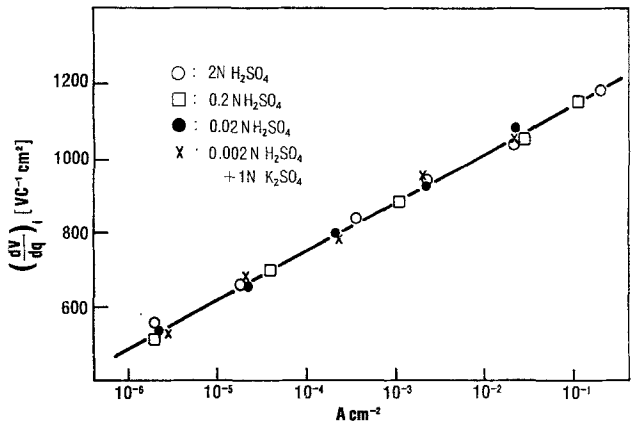

Fig. 2. Slopes of the *V-q* traces, such as those in Fig. 1, plotted against the applied current density. Data are corrected for surface roughness.

duced several times after which the solution was replaced. Then, a constant anodic current was applied to the disk electrode from a high voltage battery pack (~190V) and precision resistors in series with the disk electrode. The ring potential was kept constant at 0.4V *vs.* RHE using a commercial potentiostat so that oxygen evolved at the disk electrode could be detected at the ring electrode. The ring current observed at the longest time of polarization of the disk electrode was scaled to be equal to the current applied at the disk as essentially 100% oxygen evolution occurs at long times. In the potential region of O_2 evolution, all other currents are much smaller than that for O_2 evolution. For instance, Pt dissolution current density is about 10^{-9} A-cm^{-2} (12). The ring currents at shorter times could then be readily converted, by reference to this scale, to give the fraction of the applied disk current utilized in the O_2 evolution. For this scaling, it does not matter whether O_2 is reduced to H_2O or to H_2O_2, providing the ratio of the currents for these partial processes is constant during measurements. With the gold ring electrode in acid solutions, H_2O_2 is the predominent product in the reduction (11, 13), and this is reflected in lower ring currents than calculated. This is discussed below.

Both the potential at the Pt disk and the current at the Pt ring electrode were monitored with time on an X-Y-Y recorder.

Results and Discussion

Rates of the individual processes of oxide growth and oxygen evolution.—Growth of oxide film in the linear V/t region.—The relationships between V and q in the linear V/t region are given in Fig. 1 with the slopes, $\partial V/\partial q$, increasing with increasing constant current density, i, applied to the disk electrode. These slopes are found to increase linearly with log i over a few decades of current density (Fig. 2) with the same dependence being observed in acid solutions of different pH (7).

In Fig. 1, it can also be seen that the linear V/q traces intercept in extrapolation to a common point, $P(-q_o, V_o)$. The parameter q_o can be considered as the charge density equivalent to the oxygen species adsorbed at the Pt surface prior to the application of a constant current (5, 7). The parameter V_o has been found to depend on pH, decreasing 60 mV *vs.* a pH independent reference electrode as the pH increases one unit

$$V_o = V_{oo} - \frac{2.3RT}{F}\text{pH} \qquad [1]$$

This pH dependence of V_o is the cause of the shift along the V axis of the V/q traces with pH. V_o can also be seen to be independent of the applied current density (Fig. 1). V_{oo} is a constant that depends on the choice of the reference electrode (V_{oo} = 0.94V *vs.* NHE).

In the linear V/t region, the following relationships hold

$$\frac{\partial V}{\partial q} = \frac{1}{\alpha}\ln\frac{i}{i_o} = f(i_{disk}) \qquad [2]$$

and

$$\frac{\partial V}{\partial \ln i_{disk}} = \frac{q}{\alpha} = f(q) \qquad [3]$$

Here, i_o is the current density at which $\partial V/\partial q = 0$ (Fig. 2) and can be considered to be the exchange current density (7).

Therefore, the kinetics of Pt oxide growth in the linear V/t region can be described by the rate equation (7, 14)

$$i_{og} = i_{o,og}\exp\left[\frac{\alpha(V - V_o)}{q + q_o}\right] \qquad [4]$$

where α can be evaluated from

$$\frac{\partial^2 V}{\partial q \partial \ln i_{og}} = \alpha^{-1} \qquad [5]$$

From Fig. 2, α = 0.018 CV^{-1}-cm^{-2} and i_o is equal to 2×10^{-10} A-cm^{-2} independent of the pH. The values of i_o, q_o, and α are given with respect to the true area of the Pt electrode surface (7). In the linear V/t region, almost all the applied current density at the disk, i_{disk}, is used for oxide formation and hence $i_{disk} \simeq i_{og} \simeq i$.

The observed rate, Eq. [4], can be derived from the Cabrera and Mott model (15) of the high field-assisted growth of anodic oxide films (7, 14)

$$i_{og} = i_{o,og}\exp\left[\frac{ze\lambda(V - V_o)}{dkT}\right] \qquad [6]$$

Here, ze is the charge of ions migrating in the field and participating in the rate determining step, and λ is the half-jump distance of the ions. An analysis has shown that $(V - V_o)$ is the potential difference across the growing oxide film and the inner Helmholtz layer (16). Accordingly, V_o is the potential of the inner Helmholtz plane with respect to a pH independent reference electrode. Therefore, V_o gives a measure of the potential difference across the outer Helmholtz layer (16).

A model of the complex interface, comprised of the oxide film and the inner and outer Helmholtz layers, is suggested in Fig. 3 for two constant current densities. During oxide growth, the potential difference across the outer Helmholtz layer (OHL) remains constant (V_o = const) at all current densities. Potential difference across the inner Helmholtz layer (IHL) is also

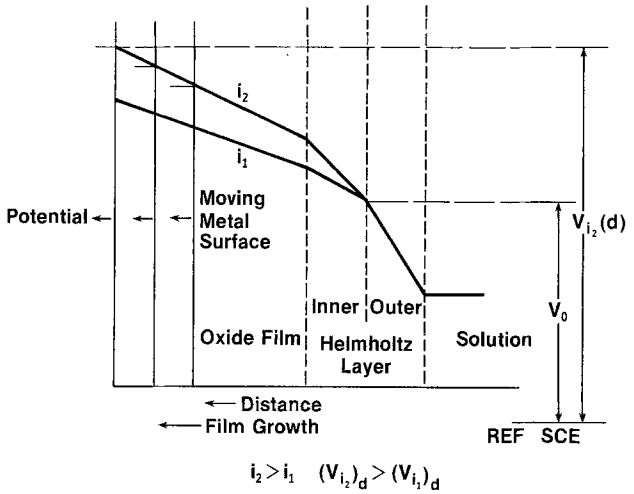

Fig. 3. A model of the interface of the oxide film and inner and outer Helmholtz layers during the oxide growth at a constant current density. Note that the potential difference across the outer Helmholtz layer is independent of applied current density.

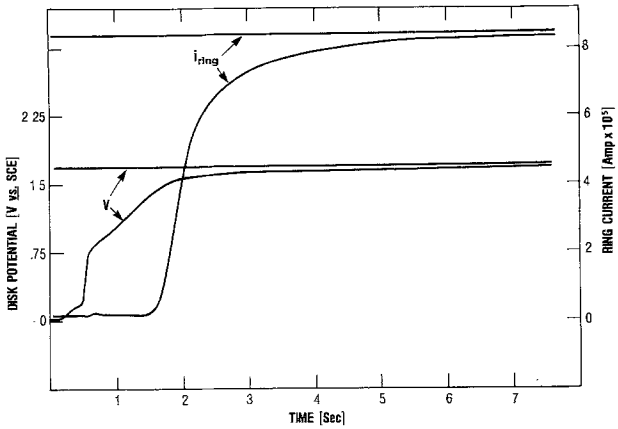

Fig. 4. Rotating ring disk electrode experiment. The ring current and the disk potential change with time. Disk current is 10^{-3} A-cm^{-2}; solution is 2*N* H_2SO_4. The ring electrode is electroplated with Au.

constant during the oxide growth at a constant current density. It decreases, however, as the current density of oxide growth increases. As the film grows at a constant current density and the metal-oxide interface propagates to the left, only the potential difference across the oxide film increases with time (and hence film thickness). However, the fields within the oxide film and the IHL remain constant during oxide growth at a given current density (16). As the current density for oxide growth decreases, these fields decrease too.

The dependence of the field in the film on the applied current density and the strength of the fields at different current densities can readily be obtained from Fig. 2 (7). For example, at 10^{-3} A-cm^{-2}, the field is about 7×10^6 V-cm^{-1}. This field is of the same magnitude as those observed for insulating anodic oxide films at valve metals (17) which shows clearly that Pt oxide films are also very poor electronic conductors.

At a constant current density, the field at any point of the complex interface (Fig. 3) should be invariant with time and thickness of the film. Therefore, it could be anticipated that the process of oxide growth would be uninterrupted and that the films would continue to thicken indefinitely as they do at valve metal electrodes. Instead, at a critical potential or a critical oxide film thickness (Fig. 1), the electrode potential ceases to increase linearly with time and O_2 begins to evolve and soon becomes the predominant reaction. In the following section, this transition from the linear *V/t* region, where oxide growth is the major reaction, to the nonlinear *V/t* region of O_2, evolution predominance is analyzed and discussed.

Growth of Pt oxide film in the transition region.— The individual rates of the oxide growth and the O_2 evolution reactions can be obtained from ring disk experiments, such as that shown in Fig. 4 for $i_{disk} = 10^{-3}$ A-cm^{-2}. The potential of the Pt disk electrode and the ring current are followed with time. The ring current is converted to give the fraction of the applied current at the disk which is utilized in the O_2 evolution reaction, i_{O_2}. Then, $i_{disk} - i_{O_2}$ gives the current due to the oxide growth reaction, i_{og}

$$i_{og} = i_{disk} - i_{O_2} \qquad [7]$$

In the linear *V/t* region (Fig. 4), no O_2 is measured at the ring electrode and essentially all of the current applied to the disk is used for oxide film formation. At the point where the linearity ceases and a charge density of about 1000 μC-cm^{-2} has passed, O_2 begins to evolve and the ring current commences to increase sharply with time (Fig. 4). However, the current at the ring electrode soon levels off and then very slowly approaches the value corresponding to 100% O_2 evolution at the disk electrode. It follows, therefore, that the current due to oxide growth is still quite significant in the transition region. In fact, after the linear *V/t* region, the film still grows an additional 30-35% for the same period of time that it grew in the linear region. Only after longer times, such as 100 sec at 1 mA-cm^{-2}, is the current at the disk due almost entirely to the O_2 evolution reaction (>99%).

It can be seen from Fig. 4 that after 15 sec, the ring current is already 8.6% of i_{disk}. After about 100 sec, the ring current reaches 9.2% of i_{disk} and remains practically unchanged with further time of polarization. At this stage, i_{disk} is used almost entirely for O_2 evolution and then i_{ring} divided by i_{disk} gives the collection efficiency of the ring electrode. In the experiment shown in Fig. 4, the ring electrode was Au-plated. Au electrodes were found to be less sensitive to residual impurities in solutions than Pt electrodes (11), and more stable ring currents were observed with these electrodes. In view of the fact that at gold electrodes O_2 is reduced mainly to H_2O_2 (11, 13), the collection efficiency is 18.4%. This value is close to the efficiency (18.2) calculated and tabulated in (18). The experimentally obtained efficiency is used to scale the ring current and calculate i_{og} according to [7].

In the nonlinear *V/t* region, the potential is again seen to increase nearly linearly with the integrated charge density for oxide film growth, $q = \int_0^t i_{og}\, dt$. This is shown in Fig. 5 for two constant current densities applied to the disk electrode. To minimize errors due to stepwise integration of small currents, the integration was carried out only up to the time when i_{ring} corresponded to about 95% i_{disk}. The dependence of *V* on *q* calculated in this way in the nonlinear *V/t* region is quite different from that in the initial linear *V/t* region and can be represented by Eq. [8], rather than by Eq. [2]

$$\frac{\partial V}{\partial q} = m = 270\ \text{VC}^{-1}\text{-cm}^2 \neq f(i_{disk}, q) \qquad [8]$$

It is shown below that this relationship is an approximate one and that $\partial V/\partial q$ is equal to *m* only at large values of *q*. As can be determined from the four current densities used in these experiments (10^{-4}, 3×10^{-4}, 10^{-3}, and 3×10^{-3} A-cm^{-2}), the following relationship holds at any *q* in the nonlinear *V/t* region (Eq. [3])

$$\frac{\partial V}{\partial \ln i_{disk}} = \frac{2RT}{F} \neq f(i_{disk}, q) \qquad [9]$$

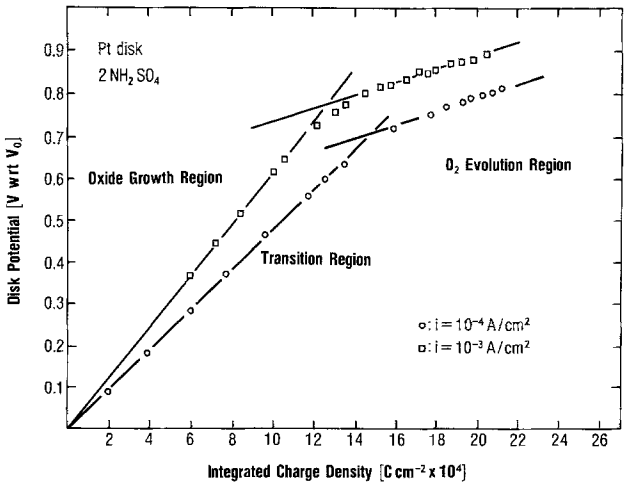

Fig. 5. Potential at the disk electrode vs. integrated charge density for oxide film growth at two current densities. Note that the V-q relationships at high q's change from those at low q's. Current and charge densities are not corrected for surface roughness (disk electrode RF = 1.4).

These relationships in the nonlinear V/t region are quite different from the corresponding relationships in the linear V/t region (Eq. [2], [3]).

To determine whether these differences in the V/q relationships in the oxide growth region and in the O_2 evolution region indicate a change in the oxide growth mechanism and/or a change in the physical properties of the film, *e.g.*, film aging and/or increasing conductivity (3), the following calculations were carried out. By using the experimentally determined values for i_{og} and q, $V - V_o$ ($=V_{calc}$) was calculated for all q by using Eq. [4] and was then compared to the observed value of $V - V_o$ ($=V_{obs}$) at each q. For this calculation, $i_{o,og}$, α, and V_o were determined from the linear V/t region for which Eq. [4] holds. The results of this comparison are shown in Fig. 6 for two applied constant current densities. It can clearly be seen that V_{calc} closely overlaps V_{obs} in all regions of the V/q curve.

It was possible to conclude from this analysis that the Pt oxide film continues to grow with the same mechanism in the transition region and in the predominantly O_2 evolution region as in the linear V/t or oxide growth region. The physical properties of the film do not change in going from the oxide growth region to the case where O_2 evolution is the major reaction. It follows then that in the O_2 evolution region, the films must still be poor electronic conductors. Furthermore, the structure of the double layer in the transition and the O_2 evolution region is basically the same as in the oxide growth region. In particular, ΔV_{OHL} remains constant, independent of the applied current density and the oxide film thickness, and has the same value as in the linear V/t region. In the nonlinear V/t region, at any constant applied current density, the fields in the film and in the IHL, however, decrease with increasing film thickness because the current density for oxide film growth continuously decreases with time or increasing film thickness. In spite of this decrease in the fields, the potential difference across the oxide film and the IHL, $(V - V_o)$, still increases with time. This is because the thickness of the film increases at a faster rate than the rate at which the field increases. This is illustrated in Fig 7. It may be noted that although the potential difference across the film and the IHL, $(V - V_o)$, increases with time, the potential difference across the IHL itself slowly decreases with time (since field decreases with time). This is discussed further below.

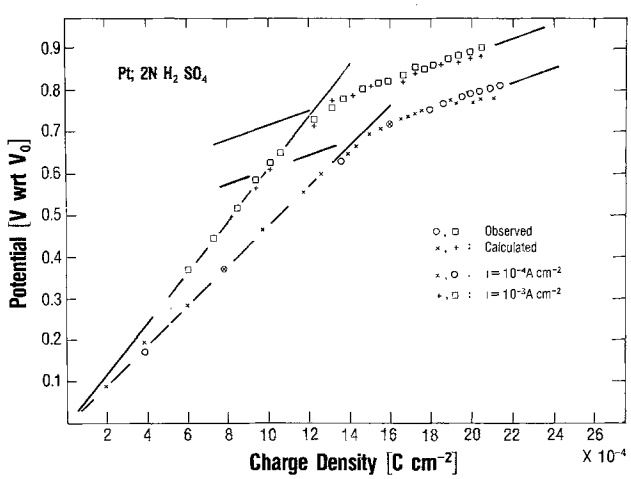

Fig. 6. Calculated and observed potentials vs. integrated charge density.

Oxygen evolution reaction in the transition region.— Once O_2 evolution becomes the predominant reaction, its rate as a function of q and V can be derived from the V/q relationships represented by Eq [8] and [9] and shown in Fig. 5 and 6. By integration of Eq. [8] and [9], the following rate equation is obtained

$$i_{O_2} = i_{o,O_2} \exp\left[-\frac{m\mathbf{F}}{2RT} q\right] \exp\left[\frac{\mathbf{F}(V - V_R)}{2RT}\right]$$

$$= i_{o,O_2} \exp\left[-\delta d\right] \exp\left[\frac{\mathbf{F}(V - V_R)}{2RT}\right] \qquad [10]$$

Here, d, the thickness of the oxide film, is equal to rq, where r ($= 9 \times 10^3$ ÅC^{-1}-cm^2) (9) converts charge density into film thickness.[1] The parameter δ is then equal to $m\mathbf{F}/(2RTr) = 0.6$ Å^{-1}. The integration constant, V_R, is chosen to be the reversible potential for the oxygen evolution reaction. The electrode potential, V, increases with time in the same way as does the potential difference, $V - V_o$, across the oxide film and the IHL. Irrespective that at a constant applied current density the potential difference across the IHL decreases gradually and ever so slowly with time, as discussed above, the current density for O_2 evolution still increases with time. This is because the current density for O_2 evolution depends on the potential difference across the oxide film and the IHL,

[1] For the $Pt(OH)_2$ structure, a monolayer of the oxide film corresponds to about 170 μC-cm^{-2}. If it is assumed that a monolayer is 2Å thick, the r factor would be somewhat higher (11.8×10^3 AC^{-1}-cm^2) than calculated from the density of $Pt(OH)_2$ (2, 9).

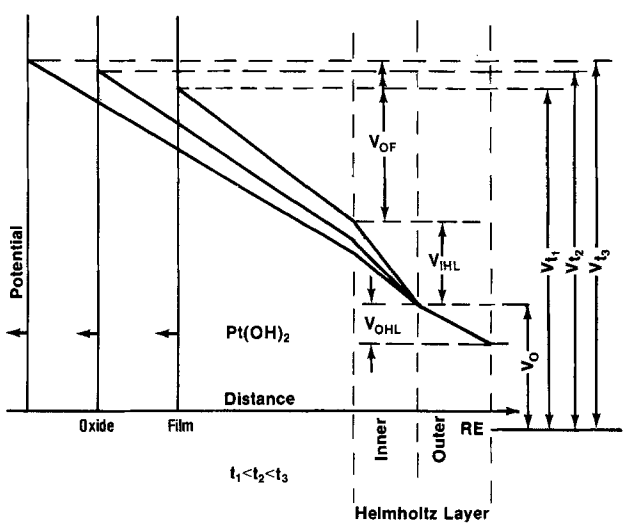

Fig. 7. A simple model of potential distribution across the oxide film and inner and outer Helmholtz layers when O_2 evolution becomes significant. Though field in the film decreases, overall potential still increases with time.

$V - V_0$, and not only on the potential difference across the IHL. This dependence on the potential difference across the oxide film and the IHL can be explained by a mechanism in which the first electrochemical step involving electron tunneling through the oxide films and IHL is rate determining. Both q and V increase with time, but the first exponential term in Eq. [10] increases at a faster rate than the second exponential term decreases, and hence the current for O_2 evolution increases with time.

An equation identical to Eq. [10] has been obtained previously from steady-state Tafel line measurements which were obtained after the initial polarization of an electrode at a constant potential or current density higher than the potentials at which the Tafel relationships were subsequently obtained (9, 19, 20). In this way, the films became fairly thick but their thickness, as determined by ellipsometry (9), remained constant during the Tafel measurements. From the ellipsometric measurements, the parameter δ was determined to be 1.4 $Å^{-1}$. The discrepancy between δ obtained in this study and that obtained by ellipsometry is not clear. No special significance is, however, given here to this difference in δ's.

The pre-exponential factor, i_{o,O_2}, is the exchange current density which would be expected at zero film thickness at the reversible potential. It can be evaluated by extrapolation to $q = 0$ of the linear V/q lines from the nonlinear V/t region. Such an extrapolation for a disk current of 10^{-3} A-cm^{-2} (Fig. 6) gives $V_{q=0} = 0.545$V *vs.* V_o, where V_o is 0.94V *vs.* RHE (7). Similarly, for a disk current of 10^{-4} A-cm^{-2}, $V_{q=0} = 0.430$V *vs.* V_o. The exchange current density at zero film thickness can now be calculated by determining the current density, i_{O_2}, expected at the reversible potential for oxygen evolution, $V_R = 1.23$V *vs.* RHE. Since this potential is 0.29V positive to V_o, it follows that, at 10^{-4} A-cm^{-2}, for instance, the overpotential for the oxygen evolution reaction is 0.14V (0.43-0.29V). Since for each decade of the applied current density, the potential changes about 115 mV, i_{o,O_2} at the reversible potential is equal to 6×10^{-6} A-cm^{-2}.

The above analysis shows that the same rate equation applies to the O_2 evolution reaction in the transition region at short times of polarization (2-10 sec at 10^{-3} A-cm^{-2}), as well as at long times (10^2-10^4 sec at 10^{-3} A-cm^{-2}). The mechanism of O_2 evolution does not change with changes in the thickness of the oxide film and with the time of polarization, and the films do not age or change their conductive properties with film thickening. However, Eq. [10] does show that the rate of O_2 evolution depends exponentially on the thickness of the oxide film. In fact, a substantial part of the overpotential for the oxygen evolution reaction arises from the effect of the barrier to charge transfer which these insulating films exert.

Oxygen evolution and oxide growth as parallel processes.—The transition from the oxide growth region to the O_2 evolution region at different current densities, such as those shown in Fig. 5, can now be understood in the following way. At any applied current density and at any q, the two processes of oxide growth and O_2 evolution, with respective partial current densities i_{og} and i_{O_2}, occur in parallel, and Eq. [7] is obeyed. These two processes depend differently on q and V (Eq. [4] and [10]). Thus for oxide growth, the V-q lines at different current densities originate at V_o and diverge linearly to infinite thicknesses and potentials. For O_2 evolution, the V-q lines are parallel and equally spaced along the potential axis for equal increments of current density. In Fig. 8, a family of diverging V/q lines, representing oxide growth at different current densities, intercept a family of parallel V/q lines, representing O_2 evolution at different current densities. When the lines for the same current density intercept, the rate of both reactions is equal.

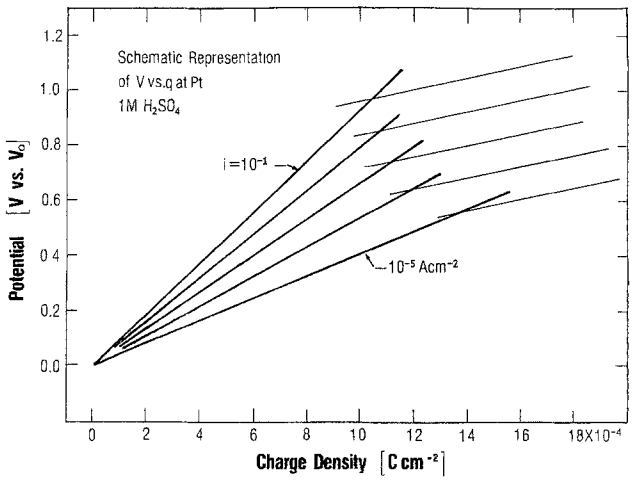

Fig. 8. Schematic representation of V-q relationships for oxide growth and O_2 evolution. At the intercepts of V-q lines for any given current density, the major process changes from oxide growth to O_2 evolution.

Quite generally, when two processes occur in parallel, the process which occurs at the lower potential, at any q, will predominate. Thus at low q, the oxide films grow with nearly 100% current efficiency. At high q, much higher potentials would be required to maintain the uninterrupted growth of the oxide films than for the evolution of oxygen. Consequently, O_2 begins to evolve and soon becomes the predominate reaction.

Figure 8 indicates that the potential of the transition points should increase while the charge density at this point should decrease with increasing applied current density. In Fig. 9, the potentials of the transition points, obtained experimentally, are plotted *vs.* the applied current density. In this figure, data of previous workers (7, 9) are included. It can be seen that the potential at the transition point does indeed increase with increasing applied current density.

Combining oxide growth and O_2 evolution in a single expression.—In the preceding discussion, it was shown that the growth of an anodic Pt oxide film obeys the same growth law (Eq. [4]) in the transition and O_2 evolution region as in the initial linear V/t region in which Pt oxide film growth is the predominant electrode reaction. Also, O_2 evolution is described by the same rate (Eq. [10]) in all regions. These equations provide the basis for the analysis of the entire V/q relationship.

The question remains as to whether the two apparently linear regions in Fig. 5 and 6 would be antici-

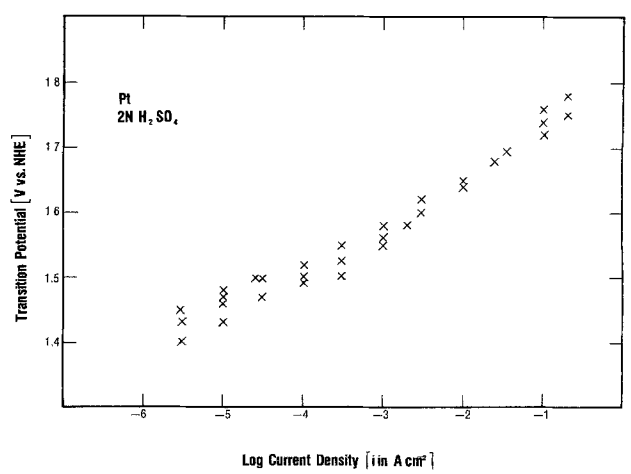

Fig. 9. Transition potentials from oxide growth to O_2 evolution in 2N H_2SO_4 as a function of applied current density.

pated to be linear by Eq. [4] and [10] when both processes occur in parallel. At any film thickness, Eq. [7] holds, and with the elimination of i_{O_2} and i_{og} from Eq. [10] and [4] by using Eq. [7], the dependence of V on q at any applied current density is readily obtained in an implicit form

$$i_{o,og} \exp\left[\frac{\alpha V}{q_T}\right] + i_{V_o,O_2} \exp\left[-\frac{mFq_T}{2RT} + FV/(2RT)\right] - i = 0 \quad [11]$$

In this equation, V is given *vs.* V_o for both the oxide growth and the oxygen evolution reaction. For this reason, i_{o,O_2} in [10] is replaced by i_{V_o,O_2} which is the current density for oxygen evolution at V_o and zero film thickness and is equal to 2×10^{-8} A-cm^{-2}. q_T represents the total charge density for oxide growth. By differentiation and by using the relationship $di_{og} = -di_{O_2}$, the following dependence of dV/dq on i_{og}, i_{O_2}, and q_T can be obtained

$$\frac{dV}{dq_T} = \frac{2RTi_{og} \ln (i_{og}/i_{o,og}) + mFq_Ti_{O_2}}{2RT\alpha i_{og} + Fq_Ti_{O_2}} \quad [12]$$

dV/dq_T continuously decreases with q_T and, therefore, neither the first nor the second V-q region should truly be linear. However, when $i_{og} >> i_{O_2}$, as in the first apparently linear V/q region, dV/dq is virtually constant for a constant current density and is given by Eq. [2]. Also, when $i_{O_2} >> i_{og}$, as in the second apparently linear V/q region, dV/dq must also become virtually constant and equal to m (Eq. [8]).

In order to estimate more accurately the degree of the linearity in both regions of the V/q plots, Eq. [11] has been calculated by computer using the experimentally determined parameters. The parameter m was determined in two ways with the first being from the slopes of the V/q traces, as discussed above. This procedure may be subject to error due to the fact that V/q traces are not expected to be quite linear. The second method for determining the value of m was by using the median value of the ring current where $i_{og} = i_{O_2}$ and where q and V are known. Then, from Eq. [10]

$$\frac{i_{disk}}{2} = i_{o,O_2} \exp\left[-\frac{mF}{2RT} q_{T,1/2} + \frac{FV_{1/2}}{2RT}\right] \quad [13]$$

where $q_{T,1/2}$, and $V_{1/2}$ are the values of q and V at $i_{og} = i_{O_2} = \frac{1}{2} i_{disk}$. With the first procedure, $m = 270$ VC^{-1}-cm^2, and with the second, $m = 330$ VC^{-1}-cm^2.

The computer-calculated V/q curve is shown in Fig. 10 and can be compared to the experimentally obtained V/q relationship as in Fig. 5. It is clear that the change of $\partial V/\partial q$ with q is negligible everywhere but near the transition point. It can therefore be concluded that a virtually linear V/q relationship exists for oxide film growth, both when the oxide growth is the predominant reaction and when the oxygen evolution is the major reaction.

Summary and Conclusions

The individual rates of Pt oxide growth and O_2 evolution at a Pt electrode in acid solutions were separated using rotating ring-disk electrode experiments. When a constant anodic current is applied to the disk electrode, the potential of the electrode is initially observed to increase linearly with time. In this linear V/t region, essentially all of the current is utilized in the formation of an insulating Pt oxide film.

Following the linear V/t region, V increases nonlinearly with time, and current at the ring electrode now commences to flow. This ring current increases sharply at first and then more slowly approaches the value expected for essentially 100% oxygen evolution. In the nonlinear V/t region, the potential is also seen to increase nearly linearly with the integrated charge density for oxide film growth.

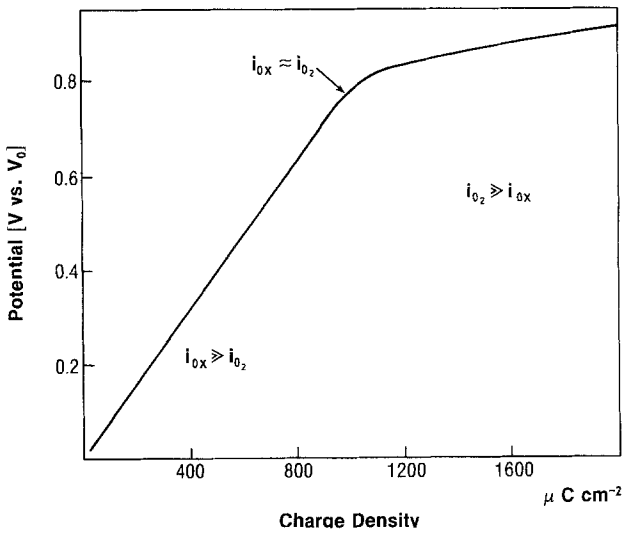

Fig. 10. Computer calculation (Eq. [11]) of V w.r.t. V_o as a function of total charge density. Note that both V/q regions are virtually linear.

In order to test the high field model for Pt oxide film growth when O_2 evolution is the major reaction, a calculation of the potential for the Pt disk electrode was made with the assumption that the mechanism of oxide growth is the same in the nonlinear V/t region as it was in the oxide growth region. It was found that the observed and the calculated potentials match closely at all values of q. Therefore, it was concluded that Pt oxide films continue to grow beyond the linear V/t region according to the same mechanism as in the linear V/t region. Consequently, the physical properties of the film, such as the electronic conductivity, do not change in going from the oxide growth region to the predominantly O_2 evolution region.

The close match between the calculated and the observed V/q curves also implies that the structure of the oxide film/solution interface remains unchanged throughout the V/q curves. In particular, the potential difference across the OHL remains constant, independent of the applied current density, and has the same value in the nonlinear V/t as in the linear V/t region.

The mechanism of the O_2 evolution reaction does not change with increasing oxide film thickness although the rate of the O_2 evolution reaction depends exponentially on the film thickness. The exchange current density for oxygen evolution at zero oxide film thickness is as high as 6×10^{-6} A-cm^{-2} compared to about 10^{-10} A-cm^{-2} at oxide-covered electrodes (19).

At any applied current, the two processes of oxide growth and O_2 evolution occur in parallel. The process which occurs at the lower potential for the same current density and oxide thickness predominates. A computer calculation of the entire V/q curve shows that virtually linear V/q relationships exist both when oxide growth is the predominant reaction and when oxygen evolution is the major reaction.

Manuscript submitted Jan. 15, 1982; revised manuscript received Jan. 11, 1983.

Any discussion of this paper will appear in a Discussion Section to be published in the June 1984 JOURNAL. All discussions for the June 1984 Discussion Section should be submitted by Feb. 1, 1984.

Allied Corporation assisted in meeting the publication costs of this article.

REFERENCES

1. M. L. B. Rao, A. Damjanovic, and J. O'M. Bockris, *J. Phys. Chem.*, **67**, 2508 (1963).
2. A. Damjanovic, A. T. Ward, B. Ulrick, and M.

O'Jea, *This Journal*, **122**, 471 (1975).
3. K. J. Vetter and J. W. Schultze, *J. Electroanal. Chem.*, **34**, 131, 141 (1972).
4. J. L. Ord and F. C. Ho, *This Journal*, **118**, 46 (1971).
5. A. Damjanovic, L-S. R. Yeh, and J. F. Wolf, *ibid.*, **127**, 1945 (1980).
6. H. Angerstein-Kozlowska, B. E. Conway, and W. B. A. Sharp, *J. Electroanal. Chem.*, **43**, 9 (1973).
7. A. Damjanovic and L-S. R. Yeh, *This Journal*, **126**, 555 (1979).
8. L. B. Harris and A. Damjanovic, *ibid.*, **122**, 593 (1975).
9. A. T. Ward, A. Damjanovic, E. Gray, and M. O'Jea, *ibid.*, **123**, 1599 (1976).
10. B. E. Conway and S. Gottesfeld, *J. Chem. Soc. Faraday Trans. I*, **69**, 1090 (1973).
11. A. Damjanovic, M. A. Genshaw, and J. O'M. Bockris, *This Journal*, **114**, 466, 1108 (1967).
12. A. N. Chemodanov, Y. M. Kolotyrkin, M. A. Dembrovskii, and T. V. Kudryavina, *Dokl. Akad. Nauk. SSSR*, **171**, 1384 (1966).
13. M. A. Genshaw, A. Damjanovic, and J. O'M. Bockris, *J. Electroanal. Chem.*, **15**, 163 (1967).
14. A. Damjanovic and A. T. Ward, in "International Review of Science; Physical Chemistry," Series II, Vol. 8, Butterworths, London (1976).
15. N. Cabrera and N. F. Mott, *Rept. Prog. Phys.*, **12**, 163 (1949).
16. A. Damjanovic, L-S. R. Yeh, and J. F. Wolf, *This Journal*, **129**, 55 (1982).
17. L. Young, "Anodic Oxide Films," Academic Press, New York (1961).
18. W. J. Albery and M. L. Hitchman, in "Ring-Disc Electrodes," pp. 22, 156, and 157, Oxford University Press, Oxford, England (1971).
19. A. Damjanovic and B. Jovanovic, *This Journal*, **123**, 374 (1976).
20. A. Damjanovic, A. T. Ward, and M. O'Jea, *ibid.*, **121**, 1186 (1974).

A Study of the Anomalous *p*H Dependence of the Oxygen Evolution Reaction at Platinum Electrodes in Acid Solutions

V. I. Birss[1]

Department of Chemistry, University of Ottawa, Ottawa, Ontario, Canada

A. Damjanovic*

Corporate Research and Development, Allied Corporaton, Morristown, New Jersey 07960

ABSTRACT

Steady-state V-log i relationships have been determined for the oxygen evolution reaction at platinum electrodes in acid solutions of various pH's. At all pH's, Tafel slopes close to $2RT/\mathbf{F}$ have been obtained after initially cathodically pretreating the electrode, polarizing it at a high anodic current density for a particular length of time, and then measuring the V-log i relationships at current densities lower than that used in the initial anodic electrode pretreatment. The order of the reaction with respect to hydrogen ions is then found to be one-half.

In other experiments, a rotating Pt ring disk electrode was used in solutions of various pH's in order to separate the currents due to Pt oxide film growth and those due to the oxygen evolution reaction and to accurately determine the charge density utilized for film growth. From this, it could be seen that the potential, at any constant charge density and pH, increases 120 mV for a tenfold increase of the current density, and that at a given current density and charge density, the potential decreases 60 mV as the pH increases one unit. These results confirm that the unusual fractional reaction order with respect to hydrogen ions is still obtained when the thickness of the oxide film remains constant. Further, it is reported here that the dependence of the oxygen evolution rates on pH can be attributed entirely to the dependence on the pH of the potential difference across the outer Helmholtz layer at the oxide film/solution interface. This simultaneous study of oxide film growth and the oxygen evolution reaction has led to a model for the potential distribution across the metal/oxide film/IHL/OHL/solution interface during the oxygen evolution reaction and to the conclusion that a fast quasi-equilibrium process exists across the outer Helmholtz layer.

The oxygen evolution reaction (OER) at platinum electrodes, in both acid and alkaline solutions, is a complex process that is still not satisfactorily understood. Evidence of this is shown by the great variance in the kinetic data of previous workers, even when apparently the same experimental conditions have been used, thus making any analysis of the reaction mechanism rather difficult. For example, in an early work, Hickling and Hill (1) reported a Tafel slope of $2RT/\mathbf{F}$ (130 mV/decade) for the OER in 1N H_2SO_4 solutions at current densities from 10^{-5} to 10^{-3} A-cm^{-2}. On the other hand, Pushnograeva *et al.* reported two different Tafel slopes for the OER in this same solution (2). For current densities of about 10^{-5}-10^{-3} A-cm^{-2}, the slope was close to $2RT/\mathbf{F}$, while for current densities from about 10^{-3}-5×10^{-2} A-cm^{-2}, the slope was close to $3RT/\mathbf{F}$ (175-190 mV/decade). Shultze and Vetter, however, reported V-log i relationships with a slope of about 120 mV/decade at low current densities but a slope of only 95 mV/decade at high current densities (3). Most other workers (4-11) have reported Tafel slopes close to $2RT/\mathbf{F}$ in acid solutions, frequently for over five decades of current density (4, 6, 7).

Part of this variance in Tafel slope determinations can be related to the lack of control of electrode pretreatment and of the procedure of V-log i measurements. It is now well documented that a thin insulating oxide film, presumably $Pt(OH)_2$ (12), grows at a platinum surface at potentials more positive than about 1.0 V/RHE (13-16). The rate of growth depends on the potential and film thickness (13-16). It is also well known that the rate of the OER depends critically on the thickness of these films (3, 9, 17) so that the current density at a given potential decreases exponentially with increasing thickness of the oxide film (3, 17).

Due to the effect of the film thickness on the kinetics of the OER, it is essential that the determination of the Tafel lines, required for a mechanistic analysis of the OER, is carried out under strictly controlled conditions of film growth or film thickness. For example, meaningful Tafel lines have been obtained when the

* Electrochemical Society Active Member.
[1] Present address: Department of Chemistry, University of Calgary, Alberta, Canada.